Review

Hybrid Additive Manufacturing via Wire Arc Metal Deposition and Deformation for Microstructure Refinement and Performance Enhancement

Ahmed Nabil Elalem and Xin Wu *

Posted Date: 3 April 2026

doi: 10.20944/preprints202604.0215.v1

Keywords: wire arc additive manufacturing; hybrid additive manufacturing; interlayer rolling; friction stir processing; hammer peening; ultrasonic vibration; dynamic recrystallization; severe plastic deformation; grain refinement; microstructure evolution; aluminum alloys; titanium alloys; nickel-based alloys

 doi:10.20944/preprints202604.0215.v1

Review

Hybrid Additive Manufacturing via Wire Arc Metal Deposition and Deformation for Microstructure Refinement and Performance Enhancement

Ahmed Nabil Elalem and Xin Wu *

Department of Mechanical Engineering, Wayne State University, Detroit, MI 48202, USA

* Correspondence: xinwu@wayne.edu

Abstract

Wire Arc Additive Manufacturing (WAAM) is a cost-effective and scalable technique for producing large metallic components; however, coarse columnar microstructures, strong crystallographic texture, and significant residual stresses limit its widespread adoption. In recent years, hybrid WAAM processes integrating deformation-based techniques have been developed to address these limitations. This review provides a comprehensive analysis of deformation-assisted WAAM, encompassing interlayer rolling, friction stir processing (FSP), hammer peening, laser shock peening, and ultrasonic vibration-assisted approaches. These hybrid techniques introduce additional thermomechanical parameters—strain, strain rate, and applied stress—that significantly influence microstructure evolution. The governing physical metallurgy mechanisms are discussed in detail, including dislocation accumulation, recovery, static and dynamic recrystallization, and severe plastic deformation. Studies from 2022 to 2025 are critically reviewed, highlighting the effectiveness of hybrid WAAM in promoting columnar-to-equiaxed grain transformation, reducing anisotropy, mitigating defects, and improving mechanical properties across aluminum, titanium, steels, and nickel-based alloys. The integration of auxiliary processes such as in-situ machining and heat treatment is also discussed. This review establishes a process-structure-property framework for hybrid WAAM and provides guidance for the development of advanced additive manufacturing systems capable of delivering near-net-shape components with microstructures and properties approaching those of wrought or forged counterparts.

Keywords: wire arc additive manufacturing; hybrid additive manufacturing; interlayer rolling; friction stir processing; hammer peening; ultrasonic vibration; dynamic recrystallization; severe plastic deformation; grain refinement; microstructure evolution; aluminum alloys; titanium alloys; nickel-based alloys

1. Introduction

Wire Arc Additive Manufacturing (WAAM), a Directed Energy Deposition (DED)-based process, has attracted growing attention as a viable technique for producing medium- to large-scale metallic components with high deposition rates and excellent material utilization. Compared with powder-based additive manufacturing, WAAM offers advantages in cost efficiency, scalability, and deposition speed, making it particularly attractive for aerospace, marine, energy, and tooling applications [1–4]. Despite these advantages, conventional WAAM is associated with several metallurgical and geometric limitations that restrict its broader industrial adoption.

A primary challenge in WAAM is the formation of coarse columnar grains aligned along the build direction, driven by steep thermal gradients and epitaxial solidification during layer-by-layer deposition. These columnar structures are typically accompanied by strong crystallographic textures, leading to pronounced mechanical anisotropy and reduced structural reliability [5–7]. Repeated thermal cycling and high heat input promote residual stress accumulation, which can result in

 doi:10.20944/preprints202604.0215.v1

distortion, cracking, and reduced fatigue performance [8–10]. Process-induced defects—including porosity, lack of fusion, and surface waviness—further degrade component quality and necessitate extensive post-processing [11–13].

To overcome these limitations, significant research has been directed toward hybrid WAAM processes that integrate mechanical deformation, and in some cases subtractive machining, into the additive manufacturing workflow. Deformation-assisted techniques—including interlayer rolling, hammer peening, FSP, and ultrasonic vibration—introduce controlled plastic strain during or between deposition passes, promoting grain refinement, texture randomization, defect closure, and improved mechanical performance [14–18].

Hybrid WAAM approaches have demonstrated the ability to activate fundamental metallurgical mechanisms such as dynamic recrystallization (DRX) and severe plastic deformation (SPD). Interlayer rolling introduces sufficient stored strain energy to promote recrystallization during subsequent thermal cycles, leading to fine equiaxed grain structures and reduced anisotropy [19]. FSP applied to WAAM deposits eliminates porosity and produces ultrafine grains through intense shear deformation and DRX [20]. Ultrasonic vibration-assisted WAAM, where acoustic cavitation and streaming effects enhance melt pool convection and nucleation, has also shown promising grain refinement results [21,22].

This review provides a unified framework for understanding deformation-assisted WAAM, focusing on hybrid processing strategies incorporating deformation, fundamental microstructure evolution mechanisms under different thermomechanical conditions, and their implications for mechanical performance across major alloy systems. Unlike previous reviews, this work establishes a unified thermomechanical framework explicitly linking deformation modes, processing conditions, and microstructure evolution mechanisms across multiple alloy systems, providing a systematic basis for hybrid WAAM process design and optimization.

This review is organized as follows. Section 2 introduces the fundamentals of WAAM thermophysics. Section 3 describes hybrid deposition-deformation processes. Section 4 covers alloy-specific microstructure evolution. Section 5 presents the physical mechanisms of microstructure evolution. Section 6 discusses mechanical property improvements. Section 7 addresses the integration of auxiliary processes. Section 8 presents challenges and future outlook. Section 9 provides conclusions.

2. Fundamentals of Wire Arc Additive Manufacturing and Thermophysical Characteristics

Wire Arc Additive Manufacturing is a Directed Energy Deposition process that uses an electric arc as a heat source and a continuously fed metallic wire as feedstock. It is typically implemented using gas metal arc welding (GMAW), gas tungsten arc welding (GTAW), or plasma arc welding (PAW) variants, including advanced modes such as Cold Metal Transfer (CMT) and pulsed arc techniques. The thermophysical characteristics of WAAM are governed by high heat input, relatively low cooling rates, and steep directional thermal gradients, which collectively dictate solidification behavior and microstructure evolution.

During deposition, the melt pool experiences strong thermal gradients (G) and solidification rates (R), which determine the solidification mode according to the classical G/R criterion. High G/R ratios promote epitaxial columnar growth along the maximum thermal gradient direction, typically aligned with the build direction. Consequently, WAAM components frequently exhibit coarse columnar dendritic microstructures with pronounced crystallographic textures, particularly <100> or <110> orientations in cubic alloys [23–25].

Repeated thermal cycling inherent to WAAM further complicates microstructure evolution. Each newly deposited layer reheats previously solidified material, leading to complex thermal histories characterized by partial remelting, solid-state phase transformations, and cyclic recovery processes. These cycles can result in heterogeneous microstructures, including banded structures, heat-affected zones, and variations in grain size and morphology along the build height [26–28].

 doi:10.20944/preprints202604.0215.v1

From a thermomechanical perspective, WAAM generates significant residual stresses due to non-uniform thermal expansion and contraction. Tensile residual stresses, particularly in the longitudinal direction, can lead to distortion, cracking, and reduced fatigue performance [29–31]. In addition, WAAM is susceptible to process-induced defects including porosity and surface irregularities such as waviness and stair-stepping. These defects act as stress concentrators and can significantly degrade mechanical performance under cyclic loading [32–34]. Advanced process control strategies have been shown to reduce defect formation and improve microstructural uniformity; however, purely thermal control approaches are often insufficient to eliminate columnar grain growth and anisotropy, necessitating deformation-based hybrid processing strategies [35–37].

3. Hybrid WAAM Processes with Interlayer Deformation

Hybrid WAAM processes incorporate controlled plastic deformation into the layer-wise deposition sequence to modify both solidification behavior and subsequent solid-state microstructure evolution. Unlike conventional WAAM, where microstructure is primarily governed by thermal gradients and cooling rates, hybrid approaches introduce an additional degree of freedom through strain, strain rate, and stress, enabling thermomechanical control of grain structure, defect evolution, and residual stress state. The effectiveness of these processes arises from the interplay between strain-induced defect generation and thermally activated restoration mechanisms, including recovery and recrystallization.

Deformation mechanisms in hybrid WAAM can be broadly categorized by mode of strain application: compressive deformation (e.g., interlayer rolling), which introduces relatively uniform plastic strain across the deposited layer; localized impact deformation (e.g., hammer peening and ultrasonic impact), which generates high strain rates and near-surface plastic deformation; severe plastic deformation (e.g., FSP), characterized by intense shear deformation and large accumulated strains; and oscillatory or high-frequency deformation (e.g., ultrasonic vibration), which introduces cyclic stresses and modifies melt pool dynamics and solidification behavior. Each mode results in distinct strain distributions, strain rates, and thermal-mechanical interactions, leading to different microstructural outcomes.

3.1. Interlayer Rolling: Compressive Thermomechanical Processing

Interlayer rolling is one of the most extensively studied hybrid WAAM techniques, characterized by the application of compressive plastic deformation using rollers immediately after or between deposition passes. The rolling process introduces relatively uniform plastic strain across the deposited bead, with strain magnitudes typically in the range of 5–30%, depending on roller geometry, applied load, and interpass temperature.

From a mechanistic standpoint, interlayer rolling increases dislocation density within the as-deposited microstructure, leading to significant strain hardening and accumulation of stored energy that serves as the driving force for subsequent recrystallization during thermal cycling. In alloys such as Ti-6Al-4V, steels, and aluminum alloys, rolling-induced deformation has been shown to disrupt epitaxial grain growth, promoting the transformation from columnar to equiaxed grain structures [34,35]. Gornyakov et al. [34] developed a coupled thermo-mechanical finite element model for in-process interlayer rolling during WAAM of a steel wall, showing that a slotted roller reduces tensile residual stress from 500 MPa to approximately 3 MPa in the 9th layer while also limiting wall widening and reducing shape distortion. Rolling also contributes to defect mitigation by mechanically closing pores and enhancing interlayer bonding, reducing lack-of-fusion defects and improving structural integrity.

 doi:10.20944/preprints202604.0215.v1

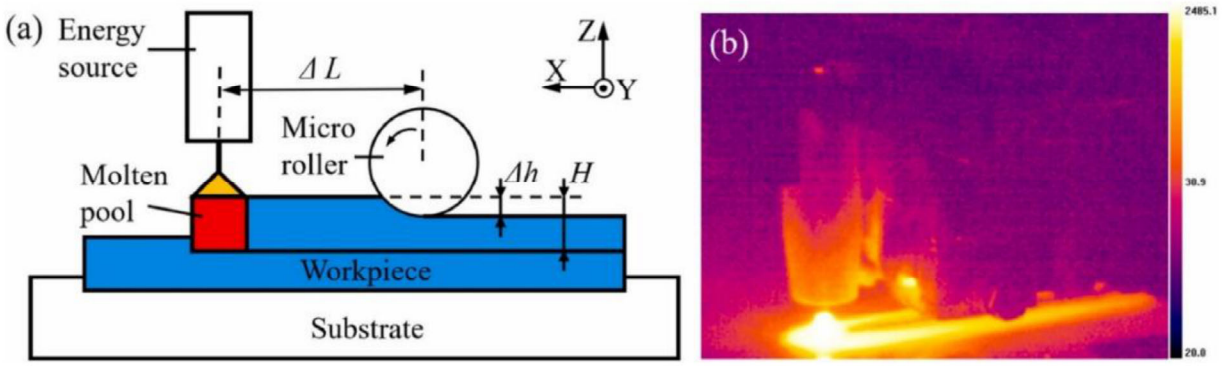

Figure 1. Hybrid interlayer hot rolling and WAAM: (a) schematic diagram; (b) temperature distribution [34]. Reprinted under a Creative Commons CC-BY-NC-ND license.

3.2. Hammer Peening and Mechanical Impact: High Strain-Rate Deformation

Hammer peening and related mechanical impact techniques introduce localized plastic deformation through repeated high-frequency impacts applied to the deposited surface. Unlike rolling, hammer peening generates high strain-rate deformation (typically 10^2 to 10^4 s^{-1}) concentrated in the near-surface region. The high strain rates lead to rapid dislocation multiplication and formation of dense dislocation networks that can evolve into refined subgrain structures. A key advantage is the ability to introduce compressive residual stresses in the surface region, counteracting tensile stresses generated during WAAM deposition and significantly enhancing fatigue performance by delaying crack initiation and propagation [37,43]. Mechanical impact processes can also influence solidification behavior—impact-induced vibrations can disrupt dendritic growth and promote grain refinement, particularly in alloys with high susceptibility to hot cracking [38].

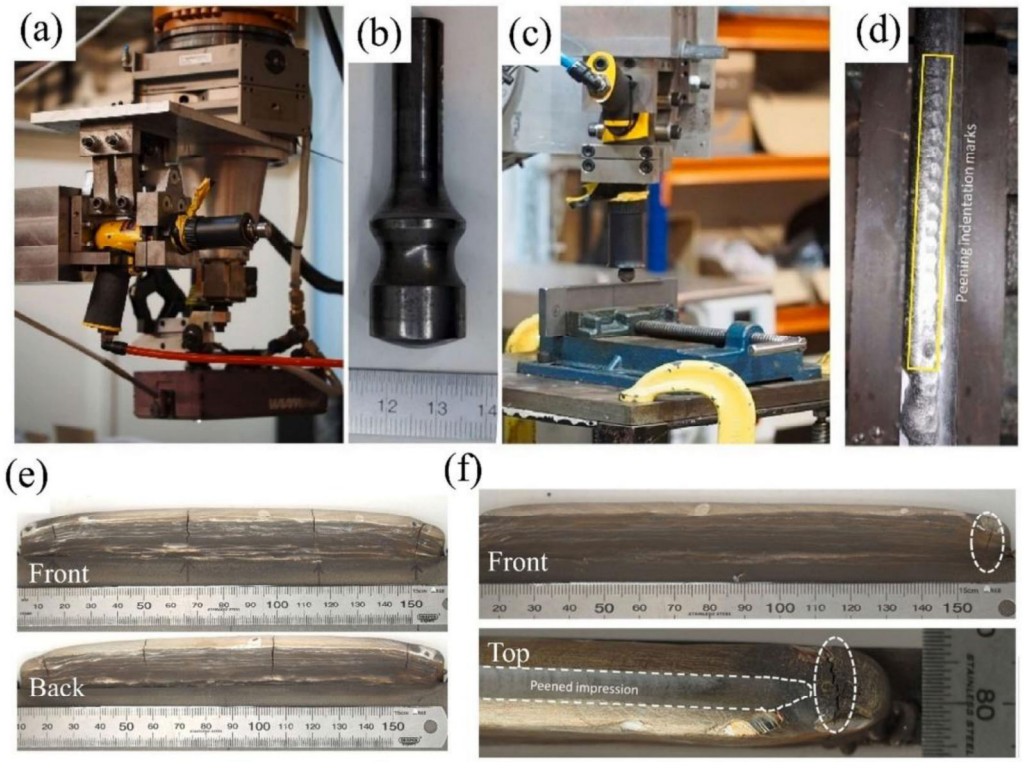

 doi:10.20944/preprints202604.0215.v1

Figure 2. MHP setup and its influence on WAAM Fe-based shape-memory alloy deposits: (a) hammer peening machine attached to Kuka robot; (b) peening tool close-up; (c) peening on the substrate surface; (d) peening indentation marks; (e) Fe-based shape memory alloy deposit showing vertical cracks; (f) front and top views of the wall fabricated with interlayer MHP-assisted WAAM. Adapted with permission from Elsevier [38].

3.3. Friction Stir Processing (FSP): Severe Plastic Deformation and Material Flow

Friction stir processing represents a severe plastic deformation technique successfully integrated into WAAM workflows. A rotating tool traversed across the deposited layer generates intense shear deformation and frictional heating. The combined effects of high strain (typically greater than 100%) and elevated temperature result in extensive microstructural modification through continuous dynamic recrystallization (CDRX), leading to the formation of ultrafine equiaxed grains, often in the range of 1–10 μm [26,27]. FSP also promotes significant microstructural homogenization—the intense material flow redistributes second-phase particles, breaks up intermetallic networks, and eliminates porosity, resulting in improved strength, ductility, and fatigue resistance. The effectiveness of FSP is highly sensitive to tool rotational speed, traverse speed, and plunge depth, which control the strain rate and temperature field that in turn determine the extent of recrystallization and grain refinement [26,61].

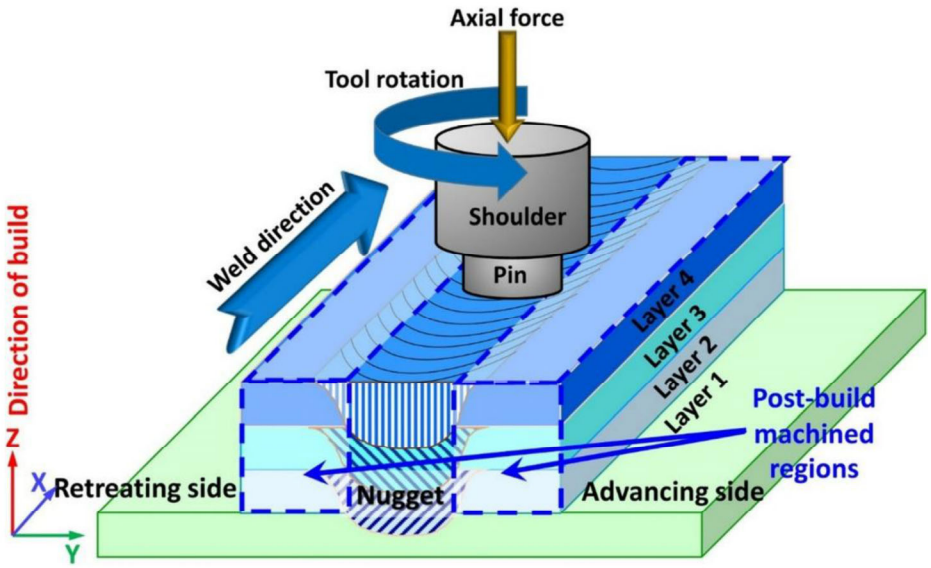

Figure 3. Schematic diagram of friction stir additive manufacturing. Adapted from Mishra and Ma (2005) [27].

 doi:10.20944/preprints202604.0215.v1

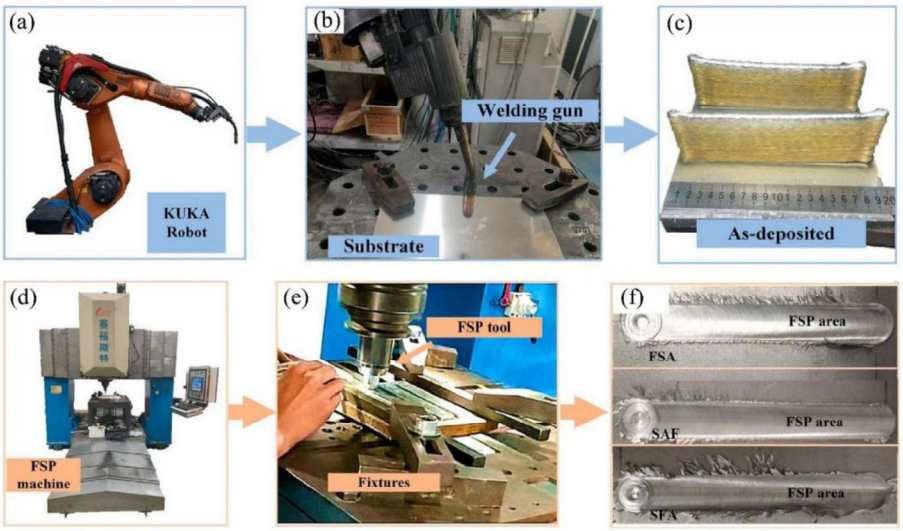

Figure 4. Process chain of WAAM followed by interlayer FSP: (a) robotic deposition system; (b) welding gun positioning during WAAM; (c) resulting as-deposited Al-Cu wall structures; (d) dedicated FSP machine; (e) tool and fixture arrangement for post-deposition stirring; (f) comparison of FSP-processed surface regions. Reprinted with permission from Elsevier [32].

3.4. Laser Shock Peening (LSP): Deep Compressive Residual Stress Induction

High-energy pulse laser beams generate plasma shock waves that propagate into the deposited layer, inducing deep compressive plastic deformation (up to 1–2 mm depth) without solid tool contact. The strain rate can be extremely high (greater than 10^6 s^{-1}) while the temperature remains near ambient. Thangamani et al. [44] studied hybrid WAAM-LSP processing of NiTi shape memory alloys and reported that LSP progressively refined grains, reduced porosity from 13.08% to 4.10%, and significantly increased UTS from 217 MPa to 426 MPa at the highest peening intensity. Sun et al. [45] demonstrated that LSP applied to WAAM-fabricated 2319 aluminum transformed tensile residual stresses into beneficial compressive stresses, resulting in greatly enhanced fatigue performance.

3.5. Ultrasonic Vibration-Assisted WAAM: Coupled Solidification-Deformation Control

Ultrasonic vibration-assisted WAAM represents an emerging hybrid processing approach that simultaneously influences liquid-phase solidification and solid-state deformation. High-frequency vibrations (typically 20–40 kHz) are introduced into the melt pool or substrate during deposition. The primary mechanisms include acoustic cavitation, acoustic streaming, and oscillatory stress fields, which collectively promote the columnar-to-equiaxed transition during solidification. Experimental studies have shown that ultrasonic vibration can significantly refine grain size in WAAM deposits, with reductions exceeding 50–80% in certain alloy systems [39,40]. The cyclic nature of ultrasonic loading can also accelerate dislocation rearrangement and promote dynamic recovery and recrystallization under appropriate conditions.

3.6. Comparative Perspective on Hybrid Deformation Techniques

Each deformation-assisted WAAM technique offers distinct advantages: interlayer rolling delivers uniform bulk deformation and effective residual stress control; hammer peening offers high strain-rate surface modification and improved fatigue resistance; FSP produces severe plastic deformation and ultrafine grain structures; LSP achieves deep compressive residual stress fields without thermal damage; and ultrasonic vibration enables coupled melt pool and solid-state control. Despite their demonstrated benefits, each technique presents inherent limitations that must be

 doi:10.20944/preprints202604.0215.v1

carefully considered based on material system, component geometry, required performance, and production constraints. Table 1 summarizes the key characteristics of each approach.

Table 1. Comparison of hybrid WAAM deformation techniques. RS = residual stress; DRX = dynamic recrystallization; SRX = static recrystallization; CDRX = continuous DRX; CET = columnar-to-equiaxed transition.

Technique	Deformation Mode	Dominant Mechanism	Microstructure Effect	Key Benefit
Interlayer Rolling	Compressive strain	DRX / SRX	Equiaxed grains	Residual stress reduction
Hammer Peening	Impact deformation	Dislocation strengthening	Surface refinement	Fatigue improvement
FSP	Severe plastic deformation	CDRX	Ultrafine grains	Homogenization
LSP	Shock/non-contact	Subsurface DRX	Deep compressive RS	Fatigue and corrosion resistance
Ultrasonic Vibration	Oscillatory + cavitation	CET + cyclic plasticity	Grain refinement	Defect reduction

4. Microstructure Evolution in Major Alloy Systems

4.1. Microstructure Evolution Mechanisms

In hybrid WAAM, the thermodynamics and physical metallurgy principles remain the same as in traditional manufacturing, but several distinctive characteristics apply. The processing zone is often highly localized, producing steep temperature and deformation field gradients. Materials experience multiple thermomechanical cycles spanning a wide domain of strain, temperature, and time, and the final microstructure is the integrated result of all cycles. The stacking-fault energy (SFE) governs the dominant deformation mechanism and post-deformation microstructural changes.

The classical metallurgical phenomena active in hybrid WAAM, in order of increasing processing temperature, are: strain hardening at low deformation temperatures (characterized by increased dislocation density and stored energy described by $E_s = \frac{1}{2}Gb^2\rho$, where G is shear modulus, b is the Burgers vector, and ρ is dislocation density); annealing (recovery) at approximately 0.2 to 0.4 Tm; static recrystallization (SRX) above approximately 0.5 Tm with sufficient prior strain, with kinetics following $X = 1 - \exp[-(kt)^n]$; and dynamic recrystallization (DRX) in hot deformation above 0.5 Tm, subdivided into discontinuous (dDRX) and continuous (cDRX) variants, the latter prevalent in high-SFE metals such as aluminum.

 doi:10.20944/preprints202604.0215.v1

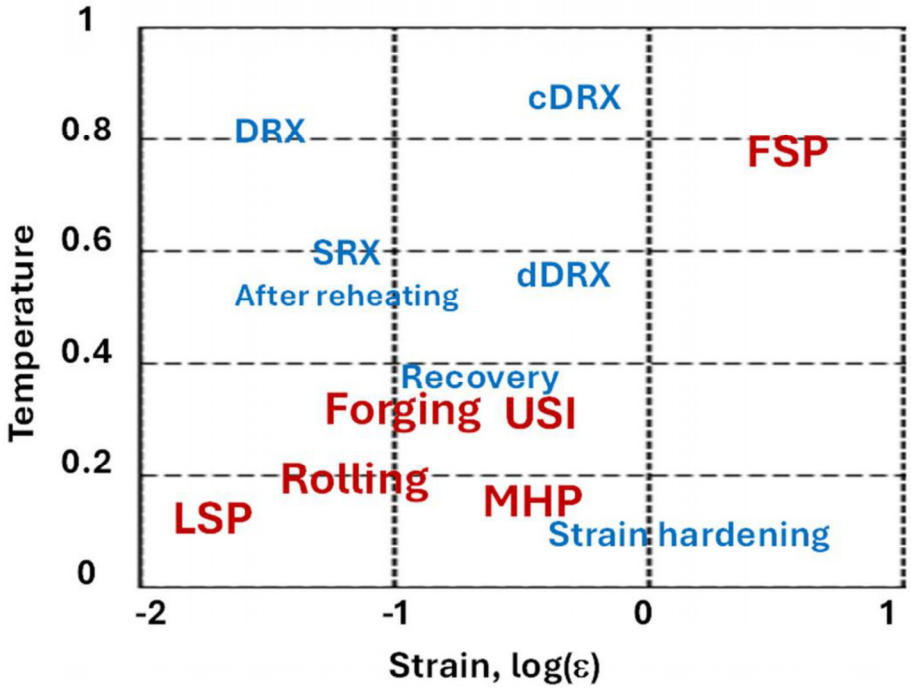

Figure 5. Schematic strain-temperature framework illustrating dominant microstructure evolution mechanisms in hybrid WAAM. Different deformation processes occupy distinct regions of the map, leading to varying contributions of strain hardening, recovery, static recrystallization (SRX), and dynamic recrystallization (DRX, d-discontinuous and c-continuous).

4.2. Aluminum Alloys

Aluminum alloys in WAAM frequently develop coarse columnar grains and high porosity due to their high thermal conductivity, fluid melt pools, and sensitivity to hydrogen pickup [52]. CMT-based WAAM walls of 2319 aluminum alloy exhibit mixed columnar and equiaxed grains with theta/theta' precipitates, retaining approximately 72% of the strength and about 65% of the fatigue strength of wrought AA2219-T62 [53,54]. Combining WAAM with interlayer FSP on 2319 aluminum generates a vertical gradient microstructure with ultrafine grains near the processed surface, increasing the DRX fraction to approximately 62% and substantially refining grains by approximately 87% [46].

The present authors (Elalem and Wu [61]) compared MIG-WAAM of 4043 aluminum alloy with a hybrid MIG-WAAM plus FSP route, in which FSP was applied behind the MIG molten pool over the deposited layer. In the WAAM-only wall, interlayer heat accumulation promoted coarse, partially dendritic grains that coarsened with build height. In contrast, MIG-FSP imposed severe plastic deformation dominated by shear strain at a high strain rate; DRX produced consistently fine equiaxed grains (a few micrometers in diameter) across all layers with a more isotropic morphology, resulting in approximately 46% higher hardness compared with the WAAM-only wall.

 doi:10.20944/preprints202604.0215.v1

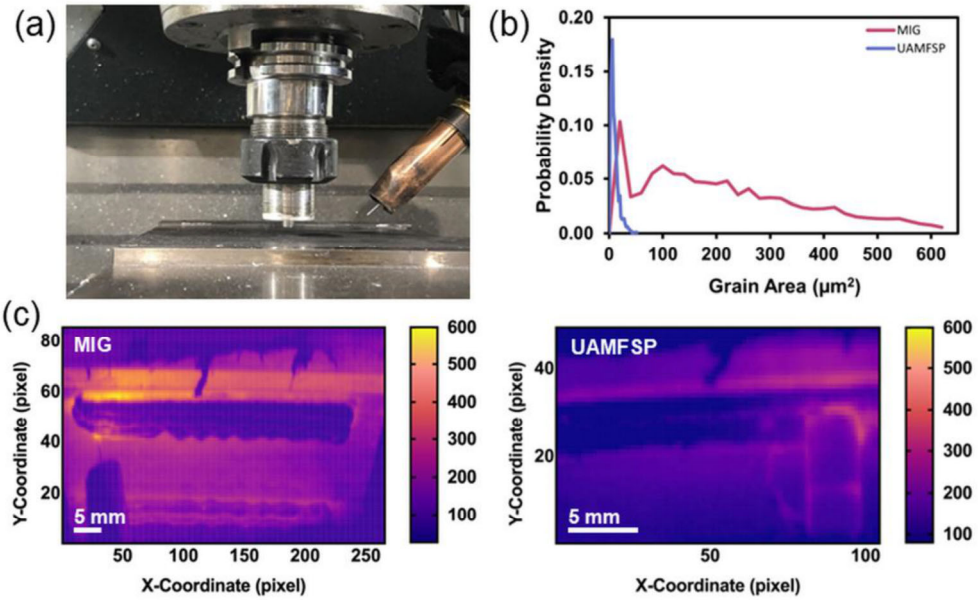

Figure 6. (a) Experimental setup consisting of MIG welder (spool gun) and FSP tool mounted on a CNC machining center (HAAS VF3); (b) comparative probability density distributions of 2D grain area for MIG only and MIG+FSP (hybrid AM), showing a strong shift toward a narrow distribution of fine grains; (c) representative infrared thermographic temperature contour maps comparing thermal fields during fabrication. Reproduced under a CC BY license [61].

Ma et al. [65] applied FSP to WAAM-fabricated 205A Al-Cu alloy, refining grains from approximately 22.8 μm to less than 5 μm, largely dissolving eutectic structures, and eliminating pore defects; FSP at 800 min^{-1} provided yield strength +32.7%, UTS +20.6%, and elongation +56.7%. Multi-pass FSP on 2319 Al walls refined grains in the stir zone to 3.4 μm [26]. For high-strength Al-Zn-Mg-Cu alloys, interlayer FSP combined with high-entropy alloy particle reinforcement achieved grain refinement to approximately 2.3 μm and simultaneous improvements in hardness (~152 HV), UTS (~374 MPa), and elongation (~10.6%) [59].

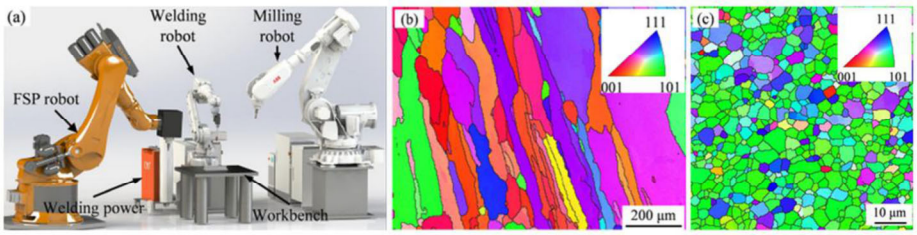

Figure 7. WAAM + FSP applied to AA6061: (a) experimental WAAM-milling-FSP robotic system; (b) EBSD inverse pole figure map of the WAAM 6061 thin-wall showing coarse columnar grains; (c) EBSD map of the WAAM + interlayer FSP stir zone showing a refined equiaxed grain structure. Adapted with permission from Elsevier [72].

 doi:10.20944/preprints202604.0215.v1

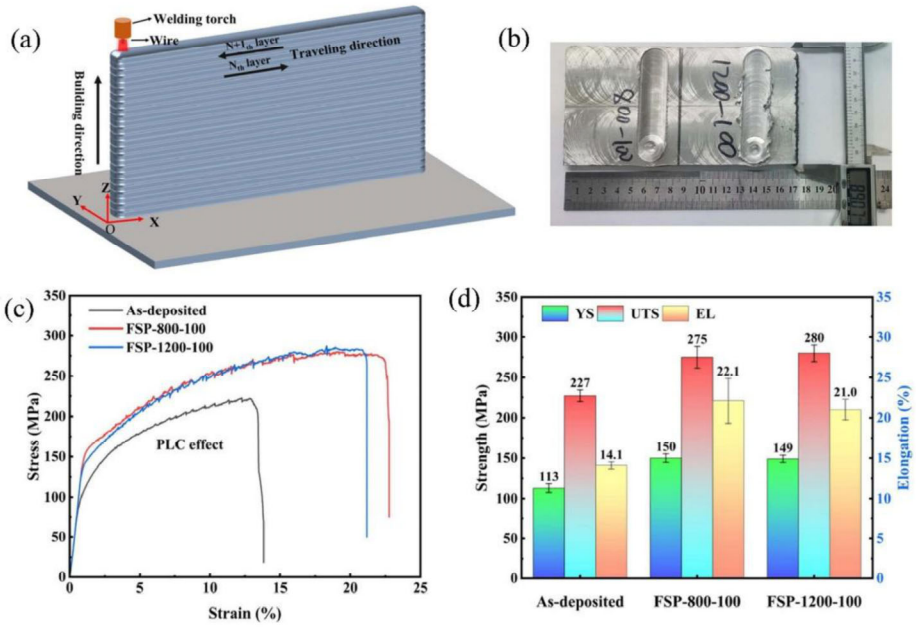

Figure 8. FSP post-treatment of WAAM-fabricated 205A Al-Cu alloy: (a) schematic of the WAAM process; (b,c) WAAM Al-Cu-Mn alloy component after FSP post-treatment; (d) stress-strain curves showing increased strength and elongation after FSP at 800 and 1200 min^{-1}; (e) comparison of YS, UTS, and elongation demonstrating substantial improvements over the as-deposited condition. Adapted under a CC BY license [65].

4.3. Titanium Alloys

Titanium alloys, particularly Ti-6Al-4V, exhibit coarse, epitaxially grown beta-columnar grains in plain WAAM, followed by martensitic alpha' or basketweave alpha formation during cooling [10]. This morphology yields pronounced anisotropy, high residual stress, and limited ductility. Maurya et al. [73] optimized a WAAM-forging hybrid route for Ti-6Al-4V, identifying a stable, high-efficiency deformation window around 900–950 °C at strain rates below 1 s^{-1}. Forging near 920 °C to strains of 0.6–0.9 significantly reduced texture intensity and improved both tensile strength and elongation. Hicks et al. [74] extended the hybrid WAAM concept to landing gear components by depositing WAAM Ti-6Al-4V features onto forged Ti-5Al-5Mo-5V-3Cr substrates, demonstrating acceptable microstructural continuity and mechanical performance. Overall, titanium alloys respond exceptionally well to deformation-assisted hybridization, with reported reductions in beta-grain width, texture intensity, and residual stress [72].

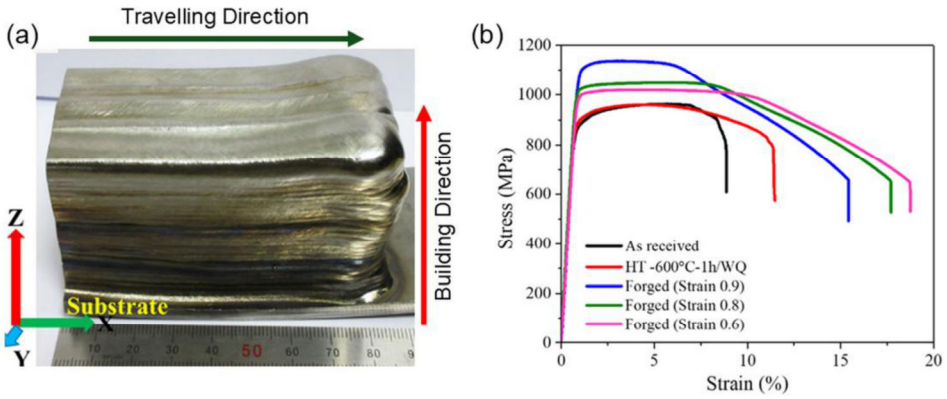

 doi:10.20944/preprints202604.0215.v1

Figure 9. (a) WAAM-built Ti-6Al-4V deposit indicating traveling direction and build direction; (b) engineering stress-strain curves comparing the as-received WAAM condition, stress-relieved state, and hot-forged conditions produced at 920 °C with imposed strains of 0.6, 0.8, and 0.9. Adapted with permission from Elsevier [73].

4.4. Steels and Stainless Steels

In steels and stainless steels, microstructure evolution during WAAM is governed by solidification mode, phase transformations, and stacking-fault energy. Plain WAAM often leads to columnar ferrite, austenite, or martensite depending on alloy content, with noticeable texture and high residual stress [13,73,74]. Panchenko et al. [77] showed that repeated reheating and slow cooling promote grain coarsening, texture sharpening, and heterogeneous hardness, confirming that poorly controlled thermal cycling can strongly degrade toughness and isotropy. Koley and Ganguly [38] demonstrated that interlayer MHP effectively suppressed hot cracking in Fe-based shape memory alloys by modifying the residual stress state and redistributing strain concentration in the solidifying weld pool. Overall, steels exhibit moderate but consistent microstructural refinement under hybrid processing, with degree of refinement generally lower than in titanium or aluminum due to higher recrystallization temperatures.

4.5. Nickel-Based Superalloys

Nickel-based superalloys such as Inconel 625 and Inconel 718 are prone to columnar solidification, segregation, Laves phase formation, and residual stress accumulation in WAAM. Their high gamma′/gamma′′ strengthening precipitate content reduces recrystallization kinetics, limiting spontaneous grain refinement during cooling [75]. Interlayer rolling introduces plastic strain that fragments the as-deposited columnar dendritic structure and, aided by reheating from subsequent deposition, promotes recrystallization to produce finer equiaxed grains. Chen et al. [78] showed that raising the solution treatment temperature from 950 °C to 1150 °C dramatically reduced the Laves phase volume fraction and re-partitioned Nb into strengthening gamma′′ precipitates, improving tensile strength and elongation by approximately 35%. Grain refinement in superalloys is often less pronounced than in titanium and aluminum due to sluggish recrystallization and high hot strength.

Table 2. Summary of deformation influence on hybrid WAAM microstructure across alloy families.

Alloy Family	As-Deposited Microstructure	Deformation Response	Key Microstructural Evolution	Key References
Al alloys	Columnar grains (often mixed), porosity/hydrogen defects, coarse intermetallic networks	High	cDRX/DRX, ultrafine/equiaxed grains; porosity elimination; improved homogeneity	[24–26,32,46,52,54,60–62,66–68]
Ti alloys	Coarse epitaxial prior-beta columnar grains; alpha′ martensite/lamellar alpha; anisotropy + residual stress	Very high	DRX/recrystallization; finer/more equiaxed microstructure; texture reduction; improved isotropy/ductility	[10,37,69–72,82]
Steels / stainless steels	Columnar ferrite/austenite/martensite; texture; residual	Moderate	Moderate grain refinement; peening/LSP near-surface refinement	[13,35,36,38,40,73,74,76]

 doi:10.20944/preprints202604.0215.v1

	stress; thermal-history sensitivity		+ compressive residual stresses	
Ni-based superalloys	Columnar gamma/dendritic solidification; segregation; Laves formation; sluggish recrystallization	Limited to moderate	Limited bulk grain refinement; rolling/FSP reduce segregation; peening/LSP deep compressive residual stress	[6,75–81,83–85]

5. Microstructure Evolution Mechanisms under Deformation-Assisted WAAM

Microstructural evolution in hybrid WAAM processes is governed by the coupled effects of temperature (T), strain (ε), strain rate ($\dot{\varepsilon}$), and applied stress (σ). A useful framework is based on the Zener-Hollomon parameter: $Z = \dot{\varepsilon} \exp(Q/RT)$, where high Z values favor work hardening and limited recovery, whereas low Z values promote dynamic restoration processes such as recrystallization.

5.1. Dislocation Accumulation, Work Hardening, and Substructure Formation

Plastic deformation introduced by hybrid WAAM generates a high density of dislocations within the crystal lattice. The evolution of dislocation density (ϱ) during deformation can be described by $d\varrho/d\varepsilon = k_1 - k_2\varrho$, where k_1 represents dislocation generation and k_2 accounts for dynamic recovery. At high strain rates or low temperatures (high Z), dislocation generation dominates, leading to rapid work hardening and the formation of dislocation cells and subgrain structures characterized by low-angle grain boundaries, which serve as precursors to recrystallized grains. Rolling and hammer peening significantly accelerate dislocation accumulation, while FSP and ultrasonic vibration can produce extremely high dislocation densities due to severe plastic deformation and cyclic loading.

5.2. Recovery, Polygonization, and Annealing

At elevated temperatures, dislocation structures undergo recovery through thermally activated processes such as climb and cross-slip, reducing stored strain energy by rearranging dislocations into more stable configurations. The rate of recovery is strongly dependent on temperature and stacking fault energy. High SFE materials (e.g., aluminum alloys) exhibit rapid recovery, while low SFE materials (e.g., austenitic steels and Ni-based alloys) retain higher dislocation densities, favoring subsequent recrystallization. In WAAM, recovery processes are frequently activated during interpass thermal cycling, resulting in partial stress relaxation and subgrain growth without fully eliminating deformation-induced heterogeneity.

5.3. Static Recrystallization (SRX)

Static recrystallization occurs when plastically deformed material is exposed to elevated temperatures without additional deformation. Its kinetics can be described by the Johnson-Mehl-Avrami-Kolmogorov (JMAK) equation: $X = 1 - \exp(-kt^n)$, where X is the recrystallized fraction, k is a temperature-dependent rate constant, and n is the Avrami exponent. In hybrid WAAM, SRX is particularly relevant when deformation is applied at relatively low temperatures, followed by reheating during subsequent deposition passes, with new strain-free grains nucleating preferentially at high-energy sites such as grain boundaries and triple junctions.

5.4. Dynamic Recrystallization (DRX): Coupled Deformation-Recrystallization Processes

Dynamic recrystallization occurs when deformation is applied at elevated temperatures, allowing recrystallization to proceed concurrently with plastic deformation. The onset of DRX is typically defined by a critical strain ($\varepsilon_c \approx 0.5\varepsilon_p$). Two primary DRX mechanisms are relevant in hybrid WAAM.

 doi:10.20944/preprints202604.0215.v1

5.4.1. Continuous Dynamic Recrystallization (CDRX)

CDRX is characterized by the gradual transformation of subgrain structures into recrystallized grains through progressive lattice rotation. This mechanism dominates in high SFE materials such as aluminum alloys and is the dominant mechanism in FSP-assisted WAAM, where large shear strains and moderate temperatures promote continuous grain refinement without distinct nucleation events.

5.4.2. Discontinuous Dynamic Recrystallization (DDRX)

DDRX involves the nucleation and growth of new grains during deformation, typically at pre-existing grain boundaries. This mechanism is common in low- to medium-SFE materials such as steels and nickel-based alloys, characterized by distinct nucleation of strain-free grains, grain boundary bulging and migration, and cyclic flow behavior in stress-strain curves. In hybrid WAAM, DDRX is often activated during high-temperature deformation processes such as interlayer rolling at elevated interpass temperatures.

5.5. Severe Plastic Deformation (SPD) and Ultrafine/Nanocrystalline Grain Formation

Severe plastic deformation occurs under conditions of very high strain ($\varepsilon \gg 1$), leading to extensive grain subdivision and the formation of ultrafine-grained or nanocrystalline structures. The relationship between grain size (d) and strength follows the Hall-Petch relation: $\sigma y = \sigma 0 + k \cdot d^{-½}$, where σy is the yield strength, $\sigma 0$ is the friction stress, and k is the Hall-Petch coefficient [47–49]. In hybrid WAAM, FSP produces ultrafine grains (1–10 μm or smaller), while hammer peening and ultrasonic impact produce nanostructured surface layers, and ultrasonic vibration can enhance grain refinement through cyclic plasticity and cavitation-assisted nucleation.

5.6. Integrated Thermomechanical Pathways and Process-Structure-Property Implications

In practical hybrid WAAM processes, these mechanisms operate simultaneously and interact dynamically. The microstructure evolution pathway depends on the local thermomechanical history: high temperature with moderate strain leads to DRX; low temperature with high strain produces dislocation accumulation followed by delayed SRX; repeated thermal cycling activates recovery and SRX; and very high strain (SPD) results in ultrafine or nanocrystalline grains. The integration of deformation into WAAM fundamentally transforms the process-structure-property relationship: grain refinement enhances strength via Hall-Petch strengthening; texture randomization improves isotropy; defect closure improves fatigue resistance; and residual stress redistribution enhances dimensional stability.

6. Mechanical Property Improvements and Performance Correlations

6.1. Strength-Ductility Synergy

In conventional WAAM, coarse columnar grains and strong crystallographic textures result in anisotropic mechanical behavior and limited ductility. Hybrid deformation processes disrupt these structures and promote equiaxed grain formation, enabling simultaneous improvements in strength and ductility. Grain refinement enhances strength through the Hall-Petch relationship, while the reduction of defects such as porosity increases the effective load-bearing area. Texture randomization reduces directional dependence of slip systems, improving uniform plastic deformation. Increases of 20–40% in yield strength and 10–30% in elongation have been reported in hybrid WAAM materials compared with as-deposited counterparts [73–76]. Zhang et al. [91] showed that inter-pass rolling improved isotropic elongation by 35–54% after heat treatment while maintaining strength through theta′/theta′′ precipitation. Zhou et al. [88] demonstrated that adding 0.15 wt.% Sc to WAAM Al-Cu walls combined with interlayer FSP increased UTS from 256 MPa to 303 MPa after FSP.

 doi:10.20944/preprints202604.0215.v1

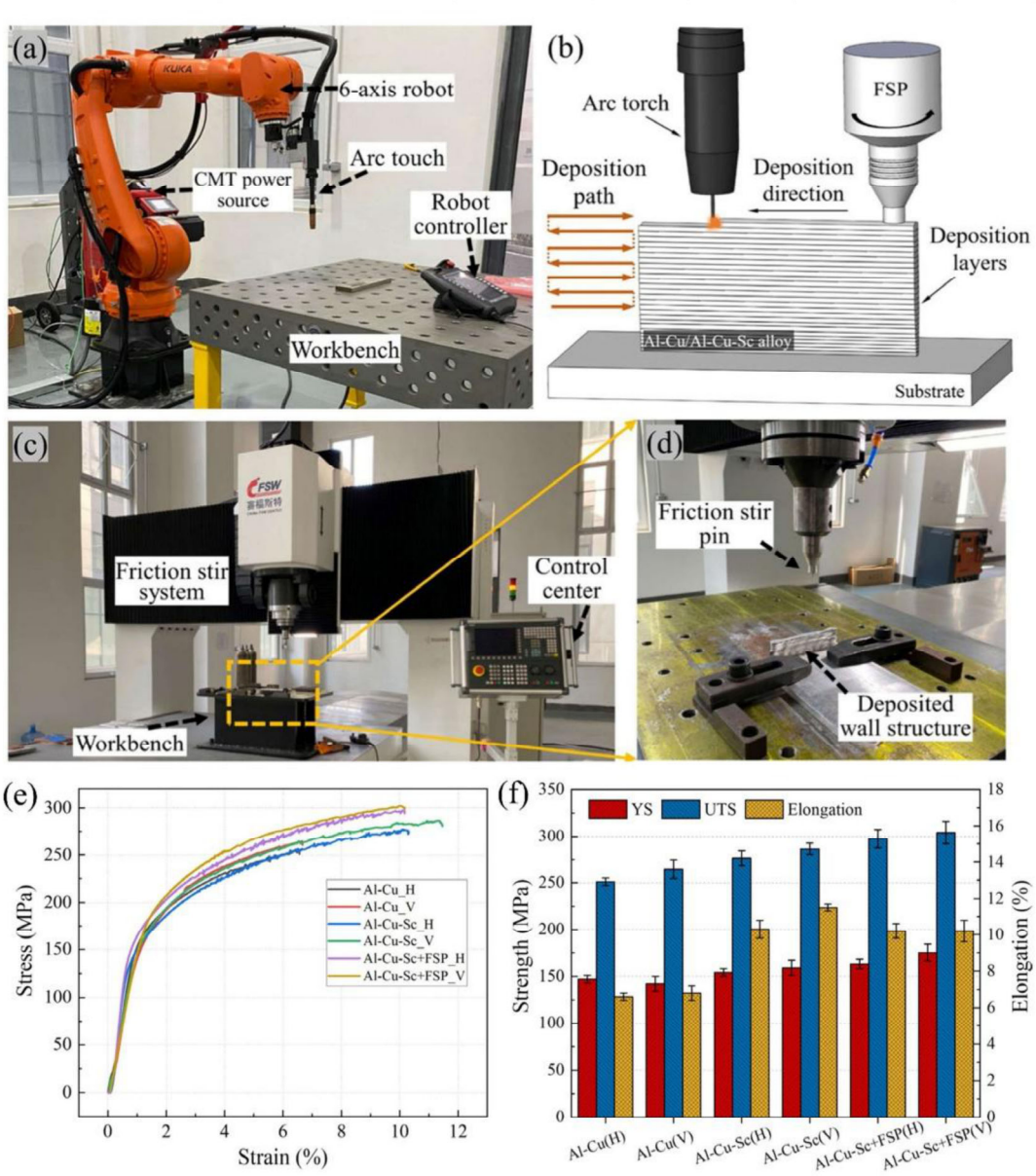

Figure 10. (a) CMT platform; (b) schematic of deposition strategy for WAAM + FSP; (c,d) FSP system; (e) stress-strain curves; (f) tensile strength histogram. Reprinted with permission from Elsevier [88].

6.2. Fatigue Performance

Fatigue performance in WAAM components is highly sensitive to surface condition, microstructural heterogeneity, and residual stress state. Hybrid deformation processes improve fatigue resistance through multiple mechanisms: grain refinement reduces slip localization; compressive residual stresses delay crack initiation; porosity closure removes critical stress concentrators; and surface integrity is enhanced through deformation-assisted smoothing. Interlayer rolling and hammer peening have been shown to significantly improve fatigue life in titanium and aluminum alloys by introducing beneficial compressive residual stresses and refining surface microstructure [37,82]. Zhang et al. [83] showed that cold rolling combined with heat treatment improves fatigue life in Inconel 718 due to gamma'' precipitation and refined Laves distribution. Wang et al. [95] reported nearly isotropic fatigue crack growth behavior in hybrid additive manufactured Ti-6Al-4V ELI, with crack growth rates comparable to wrought material.

 doi:10.20944/preprints202604.0215.v1

6.3. Creep and High-Temperature Performance

Creep resistance in WAAM materials is strongly influenced by grain structure, phase stability, and defect distribution. Coarse columnar grains in conventional WAAM can accelerate creep deformation due to grain boundary sliding and anisotropic behavior. Hybrid deformation processes improve creep performance by refining grain structures, reducing segregation and second-phase instability, and eliminating defects that act as creep cavities. In nickel-based superalloys, deformation-assisted WAAM combined with heat treatment has been shown to improve high-temperature strength and reduce creep rate by stabilizing gamma'/gamma'' precipitates and reducing Laves phase content [78,85].

6.4. Reduction of Mechanical Anisotropy

Mechanical anisotropy is a critical limitation of conventional WAAM, arising from directional solidification and columnar grain growth. Hybrid deformation processes significantly reduce anisotropy by transforming columnar grains into equiaxed structures, randomizing crystallographic texture, and homogenizing phase distribution. In titanium alloys, hybrid WAAM processes have been shown to reduce anisotropy in elongation and strength to less than 5%, compared with 20–40% in conventional WAAM [10]. Table 3 summarizes representative hybrid WAAM-based studies and their key outcomes.

Table 3. Representative hybrid WAAM-based studies and their key outcomes. FSP = friction stir processing; USI = ultrasonic impact treatment; HT = heat treatment; MHP = machine hammer peening; LSP = laser shock peening; RS = residual stress; HV = Vickers hardness.

Process	Material	Key Outcomes	Ref.
FSP	Al-Mg/SiC nanocomposite	Ceramic-reinforced nanocomposite wall with refined microstructure, reduced porosity, improved strength and hardness	[24]
FSP	AA2319 (Al-Cu)	Multi-pass stirring refined grains to 3.4 μm; UTS ~193 MPa, hardness ~90 HV	[26]
FSP	Al-Cu-Sc	Sc microalloying + FSP: UTS >300 MPa, improved plasticity and reduced anisotropy	[88]
FSP	AA4043 (Al-Si)	Refined uniform equiaxed grains by DRX, hardness increased by ~46%	[61]
FSP	Al-Zn-Mg-Cu + HEA	Grain refined to ~2.3 μm; UTS ~374 MPa, elongation ~10.6%, HV ~152	[59]
Hot rolling	Al-Mg	Interlayer hot rolling homogenized strain distribution, improved	[89]

 doi:10.20944/preprints202604.0215.v1

		work-hardening and ductility	
Cold/hot rolling + HT	AA2219	Elongation increased by 35–54% after heat treatment; strength maintained	[91]
Cold rolling + HT	Inconel 718	Low-cycle fatigue life increased after aging; grain refinement and fragmented Laves phase	[83]
In-situ rolling	Al-Si	Refined primary Si and alpha-Al grains, reduced porosity, increased strength and ductility	[63]
Interlayer rolling	S355 steel	Slotted roller reduced tensile residual stress from 500 MPa to ~3 MPa in 9th layer	[34]
USI	AZ31 Mg alloy	Refined grain structure, compressive residual stresses; improved corrosion resistance, strength, fatigue life	[39]
MHP	Ti-6Al-4V	Grain refinement, transformed tensile RS to compressive; enhanced fatigue life without additional HT	[37]
Hot forging	Ti-6Al-4V	Forging at 920 °C: DRX, equiaxed alpha, weakened texture, increased strength and elongation	[73]
LSP	AA2319	Transformed tensile to compressive residual stresses; greatly enhanced fatigue life	[45]

7. Integration of Auxiliary Processes in Hybrid WAAM

7.1. Integration of Subtractive Machining

Due to the inherent characteristics of arc-based deposition, WAAM components typically exhibit limited dimensional accuracy and high surface roughness [62,81]. The present authors developed a patented ADM process and system [103] that combines WAAM with FSP and milling in one platform cell, allowing both inner and outer edge surfaces to be machined at the layer level, resolving tool accessibility problems for complex geometries and preventing accumulation of geometric inaccuracies over multiple layers [119]. Huang et al. [108] demonstrated quantitatively that as-built surface undulations reduce the fatigue endurance limit by approximately 35% and shorten fatigue

 doi:10.20944/preprints202604.0215.v1

life by approximately 60% relative to machined specimens. Table 4 summarizes the synergistic effects of post-deformation machining in hybrid WAAM.

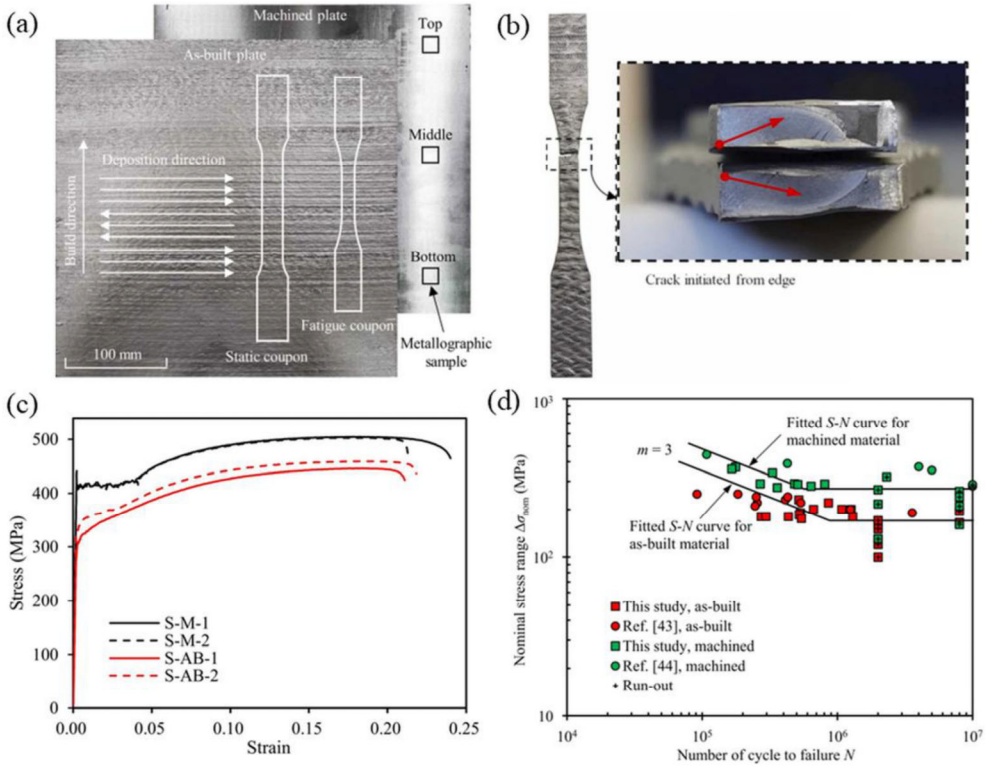

Figure 11. Effect of subtractive machining on the performance of WAAM ER70S-6 steel plates: (a) as-built and machined plate conditions and coupon extraction scheme; (b) representative fracture surface; (c) engineering stress-strain curves for machined and as-built coupons; (d) S-N comparison of as-built versus machined coupons. Adapted under a CC BY 4.0 license [108].

Table 4. Synergistic effects of post-deformation machining in hybrid WAAM.

Objective	Deformation Only	Deformation + In-Situ Machining
Grain refinement	Excellent and effective	Retained
Texture reduction	Excellent (driven by deformation)	Retained
Dimensional accuracy	Poor to moderate (bead waviness, stair-stepping)	Excellent
Surface integrity	Rough, uneven	Smooth, controlled finish
Fatigue life	Increased, but surface-dependent	Substantially increased
Residual stress state	Reduced; often more compressive near surface	Redistributed/tunable (depends on machining parameters and sequencing)

7.2. In-Situ Heat Treatment in Hybrid WAAM

Thermal management through in-situ heat treatment provides a complementary pathway for controlling phase stability, residual stress evolution, and recrystallization kinetics alongside deformation-assisted processing. In contrast to conventional ex-situ heat treatment applied after

 doi:10.20944/preprints202604.0215.v1

fabrication, in-situ thermal control occurs during or between deposition passes and is inherently coupled with the transient thermal cycles of the WAAM process. Its primary role is to regulate the balance between strain hardening, recovery, and recrystallization.

For Ti-6Al-4V, mill annealing (sub-transus, 700–785 °C) produces a fine equiaxed microstructure with superior balance of tensile strength and ductility, while beta annealing (super-transus, 1015–1050 °C) forms a lamellar microstructure that improves fracture toughness and fatigue crack growth resistance. For Inconel 718, solution treatment at approximately 980–1050 °C dissolves secondary phases, followed by two-stage aging (e.g., 720 °C then 620 °C) to precipitate gamma' and gamma'' phases. For heat-treatable aluminum alloys, T6 treatment (solutionizing, quenching, and artificial aging) maximizes strength by precipitating fine strengthening particles. Ex-situ and in-situ heat treatments are best viewed as complementary strategies: in-situ thermal control governs microstructure evolution during fabrication, while ex-situ treatments are applied selectively to optimize final properties.

8. Challenges and Future Outlook

8.1. Process Integration and Scalability

Scaling from laboratory feasibility studies to industrial-scale production remains a primary obstacle. Maintaining consistent thermal histories and uniform microstructural evolution across large build volumes is still difficult, and integrating deformation processes such as rolling, FSP, or ultrasonic vibration into large-scale WAAM systems presents challenges in equipment design, tool accessibility, and process synchronization [21,99].

8.2. Process Control, Optimization, and Closed-Loop Monitoring

Hybrid WAAM introduces additional process variables including deformation timing, strain magnitude, and temperature control. Moving from open-loop fixed parameters to closed-loop control is a critical requirement for next-generation hybrid WAAM systems. AI-driven closed-loop systems with machine learning and digital twins offer promising avenues for developing adaptive control strategies capable of responding dynamically to bead height variations, thermal fluctuations, or local microstructural conditions during the build [111,112].

8.3. In-Situ Monitoring and Defect Detection

Real-time monitoring of microstructure evolution and defect formation remains a major challenge. Techniques such as thermal imaging, acoustic emission monitoring, and laser scanning are being explored, but integration into a unified control system is still limited. Future research should focus on integrated hybrid WAAM platforms combining multiple deformation techniques; real-time closed-loop control strategies supported by machine learning and high-fidelity digital twins; expanding hybrid WAAM to emerging material systems including high-entropy alloys, advanced magnesium alloys, and functionally graded bimetallic structures; and developing standardized qualification frameworks incorporating deformation and machining steps to accelerate industrial adoption for fatigue-, creep-, and fracture-critical applications.

8.4. Extension of Materials and Hybrid WAAM Processes

High-entropy alloys (HEAs) containing five or more principal elements in near-equal composition represent a growing frontier for hybrid WAAM. Fe-Mn-Cr-Ni material systems have been processed by hybrid WAAM for in-situ alloying using multiple elemental wires, creating complex solid solutions with exceptional ductility (80% elongation) [113]. Advanced magnesium alloys also offer significant opportunity, with WAAM of scandium-modified magnesium alloys achieving yield strength of at least 200 MPa [114]. Copper alloys and bimetals present particular fabrication challenges; Joshi et al. [115] used wire WAAM to process low-alloyed steels, copper-

 doi:10.20944/preprints202604.0215.v1

aluminum alloys, and their bimetals, creating functionally graded materials for heat exchanger applications.

8.5. Toward Fully Integrated Additive-Deformation-Machining Systems

The future of hybrid WAAM lies in fully integrated manufacturing platforms that combine additive deposition, deformation processing, subtractive machining, and real-time monitoring. Such systems will enable adaptive process control, defect mitigation during fabrication, and near-net-shape manufacturing with tailored properties. Achieving this vision requires digital twins capable of predicting thermal, mechanical, and microstructural evolution in real time. The present authors' patented ADM process [103] represents one practical step toward this fully integrated vision. As standards organizations begin to include deformation and machining steps within qualification frameworks for fatigue-, creep-, and fracture-critical parts, the path toward widespread industrial adoption will become clearer.

9. Conclusions

Hybrid WAAM processes incorporating deformation-assisted techniques represent a significant advancement in additive manufacturing of metallic materials. By introducing controlled thermomechanical conditions, these processes overcome the inherent limitations of conventional WAAM, including coarse columnar microstructures, anisotropy, and defect formation. The following conclusions can be drawn from this review:

(1) Deformation-assisted WAAM processes—including interlayer rolling, hammer peening, FSP, laser shock peening, ultrasonic impact treatment, and ultrasonic vibration—provide effective and complementary pathways for microstructure refinement and defect mitigation across major alloy systems. Each technique has distinct strengths and limitations that must be considered in relation to material system, component geometry, and production scale.

(2) Microstructure evolution in hybrid WAAM is governed by coupled thermomechanical mechanisms, including dislocation accumulation, recovery, static and dynamic recrystallization, and severe plastic deformation. The Zener-Hollomon parameter provides a useful framework for predicting the operative mechanism under given deformation conditions. High-SFE alloys (e.g., aluminum) favor cDRX under FSP, while low-SFE alloys (e.g., steels and Ni-based superalloys) tend toward dDRX.

(3) Hybrid WAAM significantly improves mechanical performance, with yield strength gains of 20–40%, elongation gains of 10–30%, and substantially enhanced fatigue resistance compared with as-deposited WAAM. These improvements are mechanistically linked to Hall-Petch strengthening from grain refinement, texture randomization, porosity closure, and beneficial compressive residual stresses.

(4) Ultrasonic-assisted WAAM offers unique capabilities for simultaneously controlling solidification microstructure and introducing solid-state deformation, representing a promising direction for future research, particularly for alloys susceptible to hot cracking and hydrogen-related porosity.

(5) The integration of subtractive machining into hybrid WAAM workflows provides dimensional accuracy and surface integrity improvements that are synergistic with deformation-induced microstructural benefits, with fatigue life improvements of up to 60% demonstrated relative to as-built WAAM surfaces.

(6) Future progress requires the development of closed-loop control systems, machine learning-based process optimization, high-fidelity digital twins, and expansion of hybrid WAAM to emerging materials including high-entropy alloys, advanced magnesium alloys, and bimetallic structures. Standardized qualification frameworks incorporating deformation and machining steps are also needed to support industrial adoption.

Overall, hybrid WAAM enables the transition from purely thermal additive manufacturing to thermomechanically engineered microstructures, opening new opportunities for high-performance

 doi:10.20944/preprints202604.0215.v1

structural applications in aerospace, energy, defense, and transportation. Continued progress in process integration, monitoring, and qualification will be essential to realize the full industrial potential of this technology.

Author Contributions: Conceptualization: X.W. and A.N.E.; methodology: A.N.E.; software: A.N.E.; validation: A.N.E. and X.W.; formal analysis: A.N.E.; investigation: A.N.E.; resources: X.W.; data curation: A.N.E.; writing, original draft preparation: A.N.E. and X.W.; writing, review and editing: X.W. and A.N.E.; visualization: A.N.E.; supervision: X.W.; project administration: A.N.E.; funding acquisition: X.W. All authors have read and agreed to the published version of the manuscript.

Funding: This research received no external funding.

Acknowledgments: The authors acknowledge the support of Wayne State University and the Department of Mechanical Engineering at Wayne State University.

Conflicts of Interest: The authors declare no conflicts of interest.

Data Availability Statement: No new data were created or analyzed in this study. Data sharing does not apply to this article.

References

1. Li Y, Su C, Zhu J. Comprehensive review of wire arc additive manufacturing: hardware system, physical process, monitoring, property characterization, application and future prospects. Results Eng. 2022;13:100330.
2. Arana M, Ukar E, Rodriguez I, Iturrioz A, Alvarez P. Strategies to reduce porosity in Al-Mg WAAM parts and their impact on mechanical properties. Metals. 2021;11(3):524.
3. Chaturvedi M, Scutelnicu E, Rusu CC, Mistodie LR, Mihailescu D, Subbiah AV. Wire arc additive manufacturing: review on recent findings and challenges in industrial applications and materials characterization. Metals. 2021;11(6):939.
4. Gurmesa FD, Lemu HG, Adugna YW, Harsibo MD. Residual stresses in wire arc additive manufacturing products and their measurement techniques: a systematic review. Appl. Mech. 2024;5(3):420–449.
5. Jafari D, Vaneker THJ, Gibson I. Wire and arc additive manufacturing: opportunities and challenges to control the quality and accuracy of manufactured parts. Mater. Des. 2021;202:109471.
6. Madesh R, Kumar KG. Development of metallurgical and mechanical properties of nickel-based superalloy employed by wire arc additive manufacturing. J. Mater. Eng. Perform. 2024;33(13):6718–6737.
7. Singh SR, Khanna P. Wire arc additive manufacturing (WAAM): a new process to shape engineering materials. Mater. Today Proc. 2021;44:118–128.
8. Zhang H, Li R, Liu J, et al. State-of-art review on the process-structure-properties-performance linkage in wire arc additive manufacturing. Virtual Phys. Prototyp. 2024;19(1):e2390495.
9. Gao Z, Li Y, Shi H, et al. Microstructure characteristics under varying solidification parameters during CMT arc additive manufacturing of 2319 aluminum alloy. Vacuum. 2023;214:112177.
10. Kumar D, Vipin, Wattal R. Hybrid wire arc additive manufacturing techniques for Ti-6Al-4V functional components. J. Mater. Sci. 2025;60(45):22495–22530.
11. Derekar KS, Ahmad B, Zhang X, et al. Effects of process variants on residual stresses in wire arc additive manufacturing of aluminum alloy 5183. J. Manuf. Sci. Eng. 2021;144:071005.
12. Han Y. A finite element study of wire arc additive manufacturing of aluminum alloy. Appl. Sci. 2024;14(2):810.
13. Singh S, Jinoop AN, Paul CP, Prashanth KG. Effect of interlayer delay on the microstructure and mechanical properties of wire arc additive manufactured wall structures. Materials. 2021;14(15):4187.
14. Vishwanath N, Suryakumar S. Residual stress and distortion control in wire-arc additive manufacturing process through novel modular substrate. Proc. Inst. Mech. Eng. Part E. 2024;238(4):1570–1579.
15. Dias YEP, Lima JS de, Coelho GC, et al. Quality control, monitoring and techniques for surface quality optimization in wire arc additive manufacturing: a review. Rapid Prototyp. J. 2025.

 doi:10.20944/preprints202604.0215.v1

16. Fu R, Tang S, Lu J, et al. Hot-wire arc additive manufacturing of aluminum alloy with reduced porosity and high deposition rate. Mater. Des. 2021;199:109370.
17. Gudur S, Simhambhatla S, Venkata Reddy N. Residual stress reduction in wire arc additively manufactured parts using in-situ electric pulses. Sci. Technol. Weld. Join. 2023;28(3):193–199.
18. Li B, Nagaraja KM, Zhang R, Malik A, Lu H, Li W. Integrating robotic wire arc additive manufacturing and machining: hybrid WAAM machining. Int. J. Adv. Manuf. Technol. 2023;129(7-8):3247–3259.
19. Freitas B, Richhariya V, Silva M, Vaz A, Lopes SF, Carvalho O. A review of hybrid manufacturing: integrating subtractive and additive manufacturing. Materials. 2025;18(18):4249.
20. Kapil S, Rajput AS, Sarma R. Hybridization in wire arc additive manufacturing. Front. Mech. Eng. 2022;8.
21. Meng X, Gardner L. Hybrid construction featuring wire arc additive manufacturing: review, concepts, challenges and opportunities. Eng. Struct. 2025;326:119337.
22. Sitharaj A, Arulmurugan B, Karthi N, et al. Hybridization in metal additive manufacturing: current status and future prospectives. In: Recent Advances in Additive Manufacturing, Volume 2. Springer Nature; 2025:467–482.
23. Zhang X, He Y, Wei Y. Adopting continuous multi-pass friction stir processing to enhance the wire-arc additive manufactured ER2319 thin-walled part. CIRP J. Manuf. Sci. Technol. 2023;46:230–241.
24. Badri E, Shamsipur A, Abdollahzadeh A. AlMg/SiC nanocomposite thin wall via hybrid wire arc additive manufacturing and friction stir processing. J. Mater. Res. Technol. 2025;38:2690–2706.
25. Bagheri M, Mirsalehi SE. A novel hybrid WAAM-FSP approach for fabrication of ceramic-reinforced aluminum matrix nanocomposites. J. Alloys Compd. 2025;1042:183896.
26. Guo Y, Jiang X, Min J, et al. Microstructure evolution and grain refinement in 2319 aluminum alloy via WAAM coupled with multi-pass friction stir processing. J. Alloys Compd. 2024;1007:176338.
27. Mishra RS, Haridas RS, Agrawal P. Friction stir-based additive manufacturing. Sci. Technol. Weld. Join. 2022;27(3):141–165.
28. Li S, Zhang LJ, Zhang GF, Ning J. In-situ induce reinforcement in WAAM of Al-matrix composite using active N2 as shielding gas followed by friction stir processing. J. Mater. Res. Technol. 2024;30:1687–1695.
29. Liu L, Xu W, Li Y, et al. Effects of friction stir processing on microstructure and mechanical properties of Al-Cu alloy fabricated by WAAM. J. Mater. Res. Technol. 2025;34:539–551.
30. Liu L, Xu W, Zhao Y, et al. Tailoring the microstructure and mechanical properties of WAAM Al-Mg alloy via interlayer FSP. J. Mater. Res. Technol. 2023;25:1055–1068.
31. Nguyen DS, Song J, Fu Y, To AC. An integrated hybrid wire-arc DED, FSP, and milling system for multi-track, multi-layer part manufacturing. Addit. Manuf. Lett. 2024;11:100247.
32. Zhou S, Xu L, Wang S, et al. Effect of friction stir processing and heat treatment sequences on the microstructural evolution and mechanical properties of wire arc additively manufactured aluminum alloys. Mater. Sci. Eng. A. 2025;947:149133.
33. Huang J, Fu Y, Zhai W, et al. Hybrid interlayer hot rolling and wire arc additive manufacturing of Al-Mg alloy. J. Mater. Res. Technol. 2024;30:7037–7050.
34. Gornyakov V, Sun Y, Ding J, Williams S. Modeling and optimizing hybrid process of wire arc additive manufacturing and high-pressure rolling. Mater. Des. 2022;223:111121.
35. Lei L, Ke L, Xiong Y, et al. Microstructure, tensile properties, and fracture toughness of an in situ rolling hybrid with WAAM AerMet100 steel. Micromachines. 2024;15(4):494.
36. Xiong X, Qin X, Hua L, Wan G, Hu Z, Ni M. Microstructure evolution and parameters optimization of follow-up hammering-assisted hybrid wire arc additive manufacturing. J. Manuf. Process. 2022;84:681–696.
37. Honnige JR, Davis AE, Ho A, et al. The effectiveness of grain refinement by machine hammer peening in high deposition rate wire-arc AM Ti-6Al-4V. Metall. Mater. Trans. A. 2020;51(7):3692–3703.
38. Koley S, Ganguly S. Prevention of hot cracking in wire-arc additive manufacturing of iron-based shape memory alloy using a novel inter-layer machine hammer peening process. Mater. Sci. Eng. A. 2025;937:148453.
39. Liu X, Yin S, Zhang G, Li Y, Guan R. Effect of interlayer ultrasonic impact on the microstructure, mechanical and corrosion properties of WAAM AZ31 Mg alloy thin wall. J. Mater. Res. Technol. 2024;33:180–192.

 doi:10.20944/preprints202604.0215.v1

40. Su Z, Yang D, Yang C, et al. The influence of different ultrasonic impact treatment modes on microstructure and mechanical properties of 18Ni-300 steel fabricated by WAAM. Virtual Phys. Prototyp. 2024;19(1):e2362424.
41. Duarte VR, Rodrigues TA, Schell N, Miranda RM, Oliveira JP, Santos TG. Hot forging wire and arc additive manufacturing (HF-WAAM). Addit. Manuf. 2020;35:101193.
42. Ermakova A, Braithwaite J, Razavi N, Ganguly S, Berto F, Mehmanparast A. The influence of laser shock peening on corrosion-fatigue behavior of wire arc additively manufactured components. Surf. Coat. Technol. 2023;456:129262.
43. Xian G, Pan J, Lee J, Kang N. Weakening the anisotropic property and refining prior-beta grains via hammer peening treatment during wire arc additively manufacturing of Ti-6Al-4V. Metals. 2024;14(11):1261.
44. Thangamani G, Tamang SK, Patel MS, et al. Post-processing treatment of WAAM NiTi shape memory alloy using laser shock peening: a study on tensile behavior and fractography analysis. Int. J. Adv. Manuf. Technol. 2025;136(7):3315–3327.
45. Sun R, Li L, Zhu Y, et al. Microstructure, residual stress and tensile properties control of wire-arc additive manufactured 2319 aluminum alloy with laser shock peening. J. Alloys Compd. 2018;747:255–265.
46. Dai G, Xue M, Guo Y, et al. Gradient microstructure and strength-ductility synergy improvement of 2319 aluminum alloys by hybrid additive manufacturing. J. Alloys Compd. 2023;968:171781.
47. Segal VM. Materials processing by simple shear. Mater. Sci. Eng. A. 1995;197:157–164.
48. Segal VM. Equal channel angular extrusion: from micromechanics to structure formation. Mater. Sci. Eng. A. 1999;271:322–333.
49. Segal VM. Severe plastic deformation: simple shear versus pure shear. Mater. Sci. Eng. A. 2002;338:331–344.
50. Kennedy JR, Davis AE, Caballero AE, Williams S, Pickering EJ, Prangnell PB. The potential for grain refinement of WAAM Ti-6Al-4V by ZrN and TiN inoculation. Addit. Manuf. 2021;40:101928.
51. Rabalo MA, Garcia A, Rubio EM. Emerging trends in hybrid additive and subtractive manufacturing. Appl. Sci. 2025;15(11):6102.
52. Duan X, Cui R, Yang H, Yang X. Hybrid additive and subtractive manufacturing method using pulsed arc plasma. Materials. 2023;16(13):4561.
53. Chen Z, Liang Y, Li C, et al. Hybrid fabrication of cold metal transfer additive manufacturing and laser metal deposition for Ti6Al4V. Materials. 2024;17(8):1862.
54. Kannan AR, Pramod R, Prakash KS, Shanmugam NS, Yoon J, Oliveira JP. Understanding the microstructural evolution and fatigue behavior of aluminum 2319 fabricated by wire arc additive manufacturing. Arch. Civ. Mech. Eng. 2024;24(2):110.
55. Yuan T, Xu D, Jiang X, Chen S. Origins and optimization mechanisms of periodic microstructures in Al-Cu alloys fabricated by WAAM combined with interlayer FSP. Mater. Sci. Eng. A. 2024;916:147337.
56. Wei J, He C, Zhao Y, Qie M, Qin G, Zuo L. Evolution of microstructure and properties in 2219 aluminum alloy produced by WAAM assisted by interlayer FSP. Mater. Sci. Eng. A. 2023;868:144794.
57. Vimal KEK, Naveen Srinivas M, Rajak S. Wire arc additive manufacturing of aluminum alloys: a review. Mater. Today Proc. 2021;41:1139–1145.
58. Wei J, He C, Qie M, et al. Microstructure refinement and mechanical properties enhancement of WAAM 2219 aluminum alloy assisted by interlayer FSP. Vacuum. 2022;203:111264.
59. Shan H, Li Y, Wang S, Yuan T, Chen S. Friction stir processing of wire arc additively manufactured Al-Zn-Mg-Cu alloy reinforced with high-entropy alloy particles. J. Alloys Compd. 2025;1020:179476.
60. Dai P, Li A, Zhang J, et al. Research status and development trend of WAAM technology for aluminum alloys. Coatings. 2024;14(9):1094.
61. Elalem AN, Wu X. Process-microstructure-property characteristics of aluminum walls fabricated by hybrid WAAM with FSP. Materials. 2026;19(3):580.
62. Qie M, Wei J, He C. Microstructure evolution and mechanical properties of WAAM Al-Zn-Mg-Cu alloy assisted by interlayer FSP. J. Mater. Res. Technol. 2023;24:2891–2906.

 doi:10.20944/preprints202604.0215.v1

63. Huang J, Zhang H, Li R, et al. Hybrid in-situ hot rolling and wire arc additive manufacturing of Al-Si alloy. J. Manuf. Process. 2024;127:328–339.
64. Lv H, Bai X, Wang Y, Chen Q, Zhang H, Deng C. Submerged friction stir processing of wire arc additively manufactured Al alloy. J. Alloys Compd. 2025;1010:177351.
65. Ma J, Fan S, Gong Y, Jiang Q, Li F. Influence of friction stir processing post-treatment on the microstructure and mechanical properties of 205A aluminum alloy produced by wire arc-DED. Metals. 2025;15(3):331.
66. Wang J, Xie Y, Meng X, et al. Wire-based friction stir additive manufacturing towards isotropic high-strength-ductility Al-Mg alloys. Virtual Phys. Prototyp. 2024;19(1):e2417369.
67. Liao Z, Yang B, Xiao S, Yang G, Zhu T. Fatigue crack growth behavior of an Al-Mg4.5Mn alloy fabricated by hybrid in situ rolled wire + arc additive manufacturing. Int. J. Fatigue. 2021;151:106382.
68. Zeng L, Chen J, Li T, Tuo Z, Zheng Z, Wu H. Microstructure, mechanical properties, and fatigue resistance of an Al-Mg-Sc-Zr alloy fabricated by WAAM. Metals. 2025;15(1):31.
69. Zhou S, Wang J, Yang G, et al. Periodic microstructure of Al-Mg alloy fabricated by inter-layer hammering hybrid wire arc additive manufacturing. Mater. Sci. Eng. A. 2022;860:144314.
70. Liao Z, Yang B, Huang M, Wen W, Jiang L, Xiao S. In-situ investigation on tensile deformation behavior of hybrid hot-rolled WAAM Al-Mg alloys. J. Alloys Compd. 2025;1010:177397.
71. Elitzer D, Jager S, Holl C, et al. Development of microstructure and mechanical properties of TiAl6V4 processed by wire and arc additive manufacturing. Adv. Eng. Mater. 2023;25(1):2201025.
72. Wang F, Wei J, Wu G, Qie M, He C. Microstructural modification and enhanced mechanical properties of WAAM 6061 aluminum alloy via interlayer FSP. Mater. Lett. 2023;342:134312.
73. Maurya AK, Yeom JT, Kang SW, Park CH, Hong JK, Reddy NS. Optimization of hybrid manufacturing process combining forging and WAAM Ti-6Al-4V through hot deformation characterization. J. Alloys Compd. 2022;894:162453.
74. Hicks C, Tamimi S, Sivaswamy G, Pimentel M, McKegney S, Fitzpatrick S. Hybrid manufacturing approach for landing gear applications: WAAM Ti-6Al-4V on forged Ti-5Al-5Mo-5V-3Cr. J. Mater. Res. Technol. 2024;30:6596–6608.
75. Chen Y, Yang C, Fan C, Wang M. Microstructure evolution and mechanical properties of a nickel-based superalloy repaired using wire and arc additive manufacturing. Mater. Charact. 2022;193:112315.
76. Nagarajan S, Carter M, Curtis T, Crawford G. Cold spray-friction stir hybrid additive manufacturing of 316L SS. Mater. Des. 2025;255:114164.
77. Panchenko O, Kladov I, Kurushkin D, et al. Effect of thermal history on microstructure evolution and mechanical properties in WAAM of HSLA steel functionally graded components. Mater. Sci. Eng. A. 2022;851:143569.
78. Chen S, He Z, Xiao J, Gai S, Wang Z, Li J. Modified heat treatment and related microstructure-mechanical property evolution of arc melting additively manufactured GH4169 Ni-based superalloy. J. Alloys Compd. 2023;947:169449.
79. Zhang T, Li H, Gong H, et al. Hybrid wire-arc additive manufacture and effect of rolling process on microstructure and tensile properties of Inconel 718. J. Mater. Process. Technol. 2022;299:117361.
80. Zeng L, Wu G. Microstructure and mechanical properties of GH4169D superalloy fabricated by hybrid arc and micro-rolling additive manufacturing. Acta Metall. Sin. 2023;60(5):681–690.
81. Munther M, Martin T, Tajyar A, Hackel L, Beheshti A, Davami K. Laser shock peening and its effects on microstructure and properties of additively manufactured metal alloys: a review. Eng. Res. Express. 2020;2(2):022001.
82. McAndrew AR, Alvarez Rosales M, Colegrove PA, et al. Interpass rolling of Ti-6Al-4V wire + arc additively manufactured features for microstructural refinement. Addit. Manuf. 2018;21:340–349.
83. Zhang T, Xu W, Gong H, Wu Y, Yuan H, Su Y. Study on fatigue properties of hybrid wire arc additively manufactured and cold-rolled Inconel 718. Rapid Prototyp. J. 2025;31(8):1593–1605.
84. Pandey A, Gaur V. Interfacial characteristics of nickel-based hybrid structures fabricated using directed energy deposition. Mater. Sci. Eng. A. 2024;911:146934.
85. Hasani N, Ghoncheh MH, Kindermann RM, et al. Dislocations mobility in superalloy-steel hybrid components produced using wire arc additive manufacturing. Mater. Des. 2022;220:110899.

 doi:10.20944/preprints202604.0215.v1

86. Hosseini E, Popovich VA. A review of mechanical properties of additively manufactured Inconel 718. Addit. Manuf. 2019;30:100877.
87. del Bosque A, Fernandez-Arias P, Vergara D. Advances in the additive manufacturing of superalloys. J. Manuf. Mater. Process. 2025;9(7):215.
88. Zhou G, Huang T, Su L, Huang Q, Wu S, Zhang B. The microstructure and mechanical properties of deposited AlCuSc alloy wall structures fabricated by WAAM with FSP assistance. Thin-Walled Struct. 2025;209:112954.
89. Liao Z, Yang B, Huang M, Wen W, Jiang L, Xiao S. In-situ investigation on tensile deformation behavior of hybrid hot-rolled WAAM Al-Mg alloys. J. Alloys Compd. 2025;1010:177397.
90. Sun Z, Dai G, Ye W, et al. Modified microstructure and enhanced mechanical performance of WAAM-fabricated 2319 aluminum alloy via interlayer FSP. SSRN Preprint. 2025.
91. Zhang T, Li X, Gong H, Wu Y, Yuan H, Su Y. Investigations on microstructure and tensile properties of hybrid WAAM deposition and cold/hot rolling for 2219 aluminum alloy. Proc. Inst. Mech. Eng. Part E. 2025.
92. He C, Wei J, Li Y, et al. Improvement of microstructure and fatigue performance of WAAM 4043 aluminum alloy assisted by interlayer FSP. J. Mater. Sci. Technol. 2023;133:183–194.
93. Wei J, He C, Dong R, Tian N, Qin G. Enhancing mechanical properties and defects elimination in 2024 aluminum alloy through interlayer FSP in WAAM. Mater. Sci. Eng. A. 2024;901:146582.
94. Liu H, Yu H, Guo C, et al. Review on fatigue of additive manufactured metallic alloys. Adv. Mater. 2024;36(17):2306570.
95. Wang G, Zhang M, Fu Y, et al. Isotropy of fatigue crack growth in hybrid additive manufactured Ti6Al4V ELI titanium alloy. Mater. Sci. Eng. A. 2024;909:146850.
96. Yi M, Tang W, Zhu Y, et al. A holistic review on fatigue properties of additively manufactured metals. J. Mater. Process. Technol. 2024;329:118425.
97. Iqbal H, Pardal G, Suder W, et al. Experimental investigations on solid and metal-cored creep-resistant wires deposited under GMA and PTA-based WAAM. Int. J. Adv. Manuf. Technol. 2025;136(3):1207–1229.
98. Gornyakov V, Sun Y, Ding J, Williams S. Computationally efficient models of high pressure rolling for wire arc additively manufactured components. Appl. Sci. 2021;11(1):402.
99. Rabalo MA, Rubio EM, Agustina B, Camacho AM. Hybrid additive and subtractive manufacturing: evolution of the concept and last trends in research and industry. Procedia CIRP. 2023;118:741–746.
100. Palmeira Belotti L, van Nuland TFW, Geers MGD, Hoefnagels JPM, van Dommelen JAW. On the anisotropy of thick-walled WAAM stainless steel parts. Mater. Sci. Eng. A. 2023;863:144538.
101. Rabalo MA, Rubio EM, Agustina B, Camacho AM. Hybrid additive and subtractive manufacturing: evolution of the concept. Procedia CIRP. 2023;118:741–746.
102. Wu X, Yang Q, Elalem AN. Additive manufacturing system and unified additive-deformation-machining (ADM) process of manufacturing. US Patent 12311597B2; 2025.
103. Hu S, Wang K, Li X, Du W, Liu M, Qi J. Development and experimental validation of a hybrid wire arc additive manufacturing and milling repair platform. Int. J. Precis. Eng. Manuf. 2025;26(8):2073–2092.
104. Baumann C, Yerranagu M, Zhang W, et al. Comparison of three hybrid metal additive-subtractive manufacturing processes. CIRP Ann. 2025;74(1):321–325.
105. Campatelli G, Montevecchi F, Venturini G, Ingarao G, Priarone PC. Integrated WAAM-subtractive versus pure subtractive manufacturing approaches: an energy efficiency comparison. Int. J. Precis. Eng. Manuf.-Green Technol. 2020;7(1):1–11.
106. Zhang S, Gong M, Zeng X, Gao M. Residual stress and tensile anisotropy of hybrid wire arc additive-milling subtractive manufacturing. J. Mater. Process. Technol. 2021;293:117077.
107. Huang C, Li L, Pichler N, Ghafoori E, Gardner L. Fatigue behavior of wire arc additively manufactured sheet material. Procedia Struct. Integr. 2024;57:42–52.
108. Bagherzadeh A, Budak E, Ozlu E, Koc B. Machining behavior of Inconel 718 in hybrid additive and subtractive manufacturing. CIRP J. Manuf. Sci. Technol. 2023;46:178–190.
109. Yuan T, Xu D, Jiang X, Zhao P, Chen S. Enhanced strength-plasticity of 2319 Al-Cu alloy formed by hybrid interlayer FSP and WAAM. J. Mater. Process. Technol. 2023;321:118146.

 doi:10.20944/preprints202604.0215.v1

110. Dvorak J, Cornelius A, Corson G, et al. A machining digital twin for hybrid manufacturing. Manuf. Lett. 2022;33:786–793.
111. Tryhubov R, Kryshchuk M. Numerical modeling and digital twins in wire arc additive manufacturing. Adv. Mech. Eng. Manuf. Technol. 2025;9(3):338860.
112. Zhang X, Tong Y, Hu Y, et al. Microstructure and performance of Fe50Mn30Cr10Ni10 high-entropy alloy by wire arc additive manufacturing. Lubricants. 2022;10(12):344.
113. Yuan X-Y, Han S-J, Han L, et al. Strength and ductility synergy in Mg-11Al alloys via Sc-microalloyed dual-wire arc additive manufacturing. Mater. Res. Lett. 2026;14(3):240–249.
114. Joshi RS, Singh S, Kumar P. Wire arc additive manufacturing of low-alloyed steels, copper-aluminum alloys, and their bimetals. J. Braz. Soc. Mech. Sci. Eng. 2025;47:412.
115. Muzyk M, Pakiela Z, Kurzydlowski KJ. Generalized stacking fault energies of aluminum alloys: density functional theory calculations. Metals. 2018;8(10):823.
116. Wu X, Liu T, Cai W. Microstructure, welding mechanism, and failure of Al/Cu ultrasonic welds. J. Manuf. Process. 2015;20(3):515–524.
117. Callister WD Jr., Rethwisch DG. Fundamentals of Materials Science and Engineering: An Integrated Approach. 5th ed. Wiley; 2016.
118. Diao C, Eimer E, Mancini S, et al. Manufacture of large-scale space exploration components using wire + arc additive manufacturing. 22nd Congress of the International Council of the Aeronautical Sciences; 2022 Sep 4–9; Stockholm, Sweden.